RSC Advances

ROYAL SOCIETY OF CHEMISTRY

www.rsc.org/advances

Polyacrylonitrile-based turbostratic graphite-like carbon wrapped silicon nanoparticles: a new-type anode material for lithium ion battery

Xiaozhong Dong,[a,b] Chunxiang Lu,[a,*] Liyong Wang,[c] Pucha Zhou,[a] Denghua Li,[d] Lu Wang,[a,b] Gangping Wu[a] and Yonghong Li[a]

[a]*National Engineering Laboratory for Carbon Fiber Technology, Institute of Coal Chemistry, Chinese Academy of Sciences, Taiyuan 030001, China*

[b]*University of Chinese Academy of Sciences, Beijing 100049, China*

[c]*Department of Physics, Hebei Normal University for Nationalities, Chengde 067000, China*

[d]*Shanxi Transportation Research Institute, Taiyuan 030006, China*

Abstract

We investigated a new-type anode material of silicon (Si) nanoparticles wrapped in polyacrylonitrile (PAN)-based turbostratic graphite-like carbon, and discovered an interesting phenomenon that the battery capacity increased rather than decreased with the increase of cycling numbers. The carbonaceous matrix formed by PAN-based turbostratic graphite-like carbon could accommodate the volume change of Si nanoparticles and make the pulverized Si nanoparticles to keep good contact with the

* Corresponding author: Tel/Fax: +86 351 4166 215.

E-mail address: chunxl@sxicc.ac.cn (Chunxiang Lu).

working electrode, thus to enable the full lithiation of Si and improve the battery capacity. As a result, the capacity of the anode material reached 680 mAh g^{-1}, about twice as that of the commercial anode material, with only 9.8 w% silicon content. We also provided a new anode material preparation method that was easy to be industrialized, including using the PAN precursor and the preoxidation process to ensure the high carbon yield and the relatively high graphitization degree of the anode material. Some findings in this study are helpful to more clearly understand the lithiation-delithiation process of Si-based anode materials, as well as the basic strategy of increasing the Si-based anode material capacity.

Key words

Silicon-based anode, pulverization, turbostratic graphite-like carbon, PAN precursor, preoxidation

1. Introduction

Lithium ion batteries (LIBs) are rechargeable, green, and with high gravimetric and volumetric energy densities. The vast use of portable electronic devices, the popularization of battery-powered cars and the development of renewable energy storage systems, require LIBs with more excellent cycling performance and rate capability [1-3]. Lithium ions can intercalate to graphite quickly and reversibly, therefore, graphite materials were usually used as the anode of commercialized LIBs. Graphite anode materials have good cycling stability, however, their theoretical

specific capacity is only 372 mAh g^{-1}, which limits the further improvement of the LIB anode capacity [3-5].

In numerous researches of LIB anode materials, the theoretical capacity of silicon (Si) can reach 3579 mAh g^{-1} at room temperature. As a kind of abundant, environment-friendly electrode material, Si has a promising potential to become the next generation of LIB anode material. Unfortunately, due to the intercalation and deintercalation of lithium ions in the charge-discharge process, the volume change of Si can reach 300% at room temperature [3, 5]. This volume expansion-contraction effect of Si easily leads to the cracking and pulverization of electrode materials, and induces the contact failure with conductive collectors [3, 6, 7]. Meanwhile, it affects the formation of stable surface electrolyte interphase (SEI) films, and increases the consumption of organic electrolyte and lithium ions [1, 6, 8]. All of these factors will seriously affect the full play of the Si-based anode material performance.

Using nanoscale Si to fabricate electrode can alleviate the volume expansion-contraction effect of Si, and ease the microscopic stress and strain of Si anode materials in the charge-discharge process, such as Si nanoparticles [9], Si nanotubes [10], and Si nanowires [11]. Nevertheless, preparations of Si electrode materials with special nanostructures are complex, which are not conducive to the application of new-type electrode materials. Moreover, commercial Si nanoparticles (<100nm) still can not avoid theirs continuous pulverization during the battery use. Usually, the pulverization of Si electrode material is a negative factor to influence the

battery capacity. Considering that crystalline Si inevitably transforms to amorphous Si with the smaller size in the charge-discharge process because of the intercalation and deintercalation of lithium ions, it is necessary to find a way to turn the negative factor into positive. Another important factor to consider, the aggregation of nanoscale Si also leads to an unstable cycling performance, and affects the service life of LIBs [12]. In this study, we selected Si nanoparticles to prepare the anode material.

Carbonaceous material is light-weight, and with good conductivity. Therefore, some researchers deposited a pyrolytic carbon layer on the surface of Si nanoparticles, and increased the electrical conductivity of Si-based electrode materials, thus reduced the contact failure caused by the cracking and pulverization of electrode materials [9, 12]. At the same time, pyrolytic carbon serves as a buffer layer. The pyrolytic carbon is composed of partially graphitic and disordered carbons. The pyrolytic carbon layer with low mechanical strength can not well accommodate the expansion-contraction of Si, which partially solves the problem of the contact failure. Further, other researchers designed the core-shell structure with the carbonaceous shell and the nano-Si core, to solve the volume expansion-contraction effect of Si nanoparticles [13, 14]. The carbonaceous shell is mainly derived from organic precursor pyrolysis, and with similar but more complete structure to that of pyrolytic carbon. However, the fracture of the carbonaceous shell will happen in the charge-discharge process, due to the 300% volume expansion of the nano-Si core. The fracture of the carbonaceous shell means the formation of unstable SEI films, and the increasing consumption of organic electrolyte and lithium ions. Furthest, another part of researchers improved the

above-mentioned core-shell structure, etched Si-core materials partially or eliminated sacrifice templates by hydrofluoric acid, and obtained carbon/silicon anode materials with the yolk-shell structure, to accommodate the volume expansion of Si nanoparticles [6, 15, 16]. Si nanoparticles in the yolk-shell structure will continue pulverizing in the process of intercalation and deintercalation of lithium ions, which can not guarantee the fully contact of the carbonaceous shell and Si nanoparticles. Thereby, it limited the lithium-intercalation ability of Si nanoparticles, and influenced the cycling stability of the battery.

In order to give full play to the advantages of the carbonaceous material with good cycling stability and Si anode materials with super high lithium-intercalation ability, and inspired by the microstructure of polyacrylonitrile (PAN)-based carbon fiber—turbostratic graphite-like carbon, we designed an anode material structure with Si nanoparticles wrapped in the carbonaceous matrix. The microstructure of PAN-based carbon fiber was proved to be turbostratic graphite-like carbon [17]. The designed structure is helpful to improving the electrical conductivity of Si-based anode materials, and limiting the aggregation of Si nanoparticles. Moreover, due to high mechanical strength of PAN-based carbon, the structure in this study is robust enough to accommodate the volume change of Si nanoparticles. PAN-based carbon has not attracted more attention; the only studies are that cross-linked PAN was used as a binder during the preparation of Si-based anode electrodes [2, 18, 19].

To achieve the target of Si nanoparticles being fully wrapped in carbonaceous matrix, Si nanoparticles were firstly evenly distributed in an overdose PAN solution by mechanical stirring. PAN/Si films were prepared through the phase separation of the blend dope. Then, the PAN/Si films were preoxidized, so that PAN matrix transforms to the heat-tolerant trapezoidal structure, and to ensure that the high carbon yield and the formation of turbostratic graphite-like carbon in the following carbonization process [20]. Consequently, we obtained an anode material of Si nanoparticles wrapped in PAN-based carbonaceous matrix (Si@C).

In this study, we investigated a Si@C anode material with the structure of PAN-based turbostratic graphite-like carbon. At the same time, we provided a simple and effective material preparation method that was easy to be industrialized. We explained the phenomenon that the battery capacity increased rather than decreased, and gave the direct evidence of the pulverization of Si nanoparticles. Some findings in this study are helpful to more clearly understand the lithiation-delithiation process of Si-based anode materials, as well as the basic strategy of increasing the Si-based anode material capacity.

2. Experimental

2.1. Preparation of the Si@C Anode Material

The preparation process of the Si@C anode material is shown in Fig. 1. The PAN solution with 20% solid content was prepared through the radical polymerization in dimethyl sulfoxide (DMSO) according to the reference [21]. The obtained PAN

solution was transferred in a three-mouth flask, stirred at 50 ℃ and protected with nitrogen gas. 1g Si nanoparticles (<100nm, Xuzhou Jiechuang New Material Technology Co. Ltd., China) with a PAN/Si ratio of 20/1 (w/w) were dispersed in 30ml DMSO by ultrasonic, then slowly added into the PAN solution. A homogeneous dope was prepared by continuous mechanical stirring. After a halfhour standing, the PAN/Si blend dope was uniformly coated on the glass flake, and then immersed in the deionized water for solidification. The obtained films were washed by the 80 ℃ hot water to remove residual DMSO, and dried in the air. The dried films were cut into small strips before preoxidation. For preoxidation, the PAN/Si strips were heated to 230 ℃ at a heating rate of 3 ℃ min^{-1} and held for 50 min in a door-ajar muffle furnace [22]. For carbonization, the preoxidized strips were heated to 1000 ℃ at a same heating rate of 3 ℃ min^{-1} and held for 10 min in a tube furnace under an argon atmosphere [6, 23]. Ultimately, the carbonized strips were ground into powder for structural characterization and electrochemical tests.

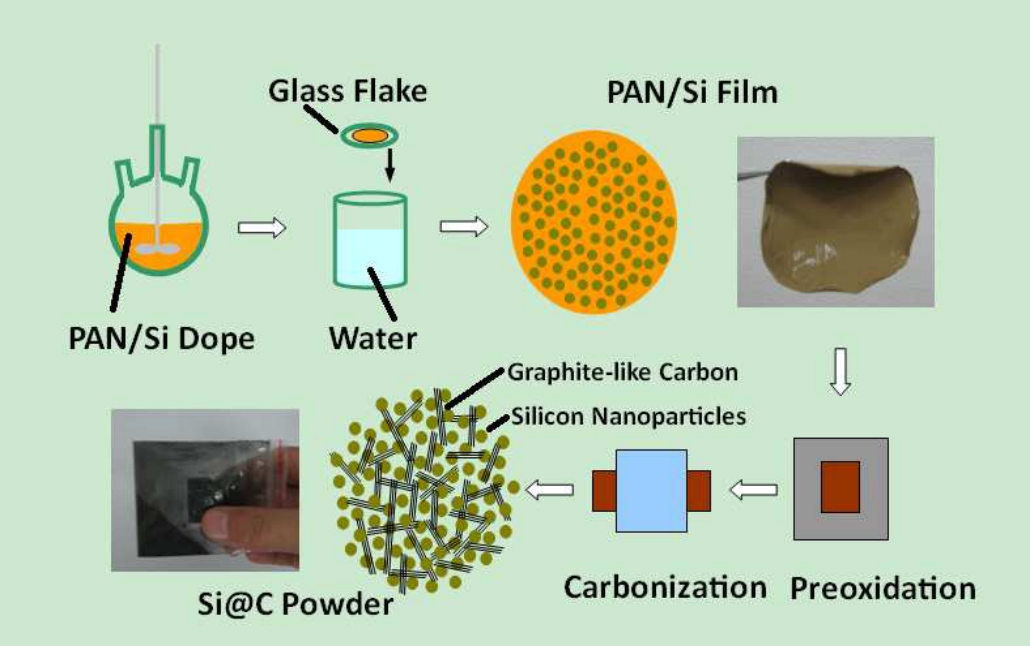

Fig. 1. The preparation process of the Si@C anode material.

2.2. Material Characterization

The prepared Si@C anode material was characterized by field-emission transmission electron microscopy (TEM, FEI Tecnai G2), x-ray diffractometer (XRD, BRUKER D8 A25), Raman spectrometer (HORIBA Scientific XPLORA), thermogravimetric analyzer (TG, Netzsch STA 409 PC/PG) and scanning electron microscopy (SEM, JSM-7001F) with energy dispersive X-ray spectroscopy (EDS).

2.3. Electrochemical Measurement

The prepared Si@C powder was firstly mixed with acetylene black and sodium carboxylmethyl cellulose in a ratio of 7/2/1 (w/w/w), and made into the working electrode. The mixed anode material loading on the copper collector is 0.98 mg cm^{-2}. Then, the working electrode was used to assemble the CR2016-type coin cell in an

argon-filled glovebox, using lithium foil as the counter electrode and reference electrode, microporous polypropylene film (Celgard2400) as the separator, and 1 M LiPF6 in ethylene carbonate/dimethyl carbonate (1/1 by volume) plus 5% volume vinylene carbonate as the electrolyte [24]. The cyclic voltammetry (CV) test of the working electrode was scanned at 1 mV s^{-1} in a voltage range of 0.01~2.0 V on an electrochemical workstation (Chenhua CHI 660E). The electrochemical impedance spectroscopy (EIS) was recorded from 10^5 to 0.01 Hz on the same workstation. By a battery test system (Jinnuo LAND CT 2001A), the cells were galvanostatically discharged and charged in a voltage range of 0.01~2.0 V at room temperature. The specific capacity was based on the total mass of Si@C.

3. Results and discussion

Fig. 2 is the characterization of the prepared Si@C anode material. As shown in Fig. 2a, Si nanoparticles (darker parts) are completely wrapped in PAN-based carbonaceous matrix (brighter parts). The arrows in Fig. 2b show PAN-based turbostratic graphite-like carbon. Fig. 2c presents the anode material structure of Si wrapped in turbostratic graphite-like carbon in the whole. Fig. 2d and 2e are details of Fig. 2c with enlarged scale. The structure shown in Fig. 2c can be further referred to Fig. S1 with more obvious lattice fringes. The interplanar distance of Si (d_{Si}) is 0.29nm in Fig. 2d, and the distance indicated by the arrows is $10d_{Si}$. While, the interplanar distance of turbostratic graphite-like carbon (d_C) is 0.35nm in Fig. 2e, and the distance indicated by the arrows is $3d_C$.

In Fig. 2f, the XRD peak of Si (111) corresponds to the 2θ angle of 28.3°. According to the Bragg equation $2d \sin\theta = n\lambda$, and $\lambda = 0.15406$ nm, the d_{Si} calculated is 0.31nm. This result is consistent with the d_{Si} in the TEM image of Fig. 2d, therefore, it can be determined that darker parts in TEM images are Si nanoparticles. The C (002) peak next to the Si (111) peak corresponds to the 2θ angle of about 25.0°. The d_C calculated through the Bragg equation is 0.36nm, consistent with the d_C of graphite-like carbon in the TEM image of Fig. 2e, and brighter parts in TEM images are determined as graphite-like carbon. Compared with carbon nanocoils [24] treated by graphitization (2800 ℃, d_C = 0.34nm), the carbonaceous matrix only treated by carbonization (1000 ℃) in this study, obviously has a dispersing C (002) peak, which indicated the existence of the turbostratic structure. The C (002) spacing of the carbonaceous matrix is bigger than that of carbon nanocoils, also in accord with the experimental condition of the 1000 ℃ carbonization process. Combined with Fig. 2d and 2e, the lattice fringes of PAN-based turbostratic graphite-like carbon developed relatively perfect.

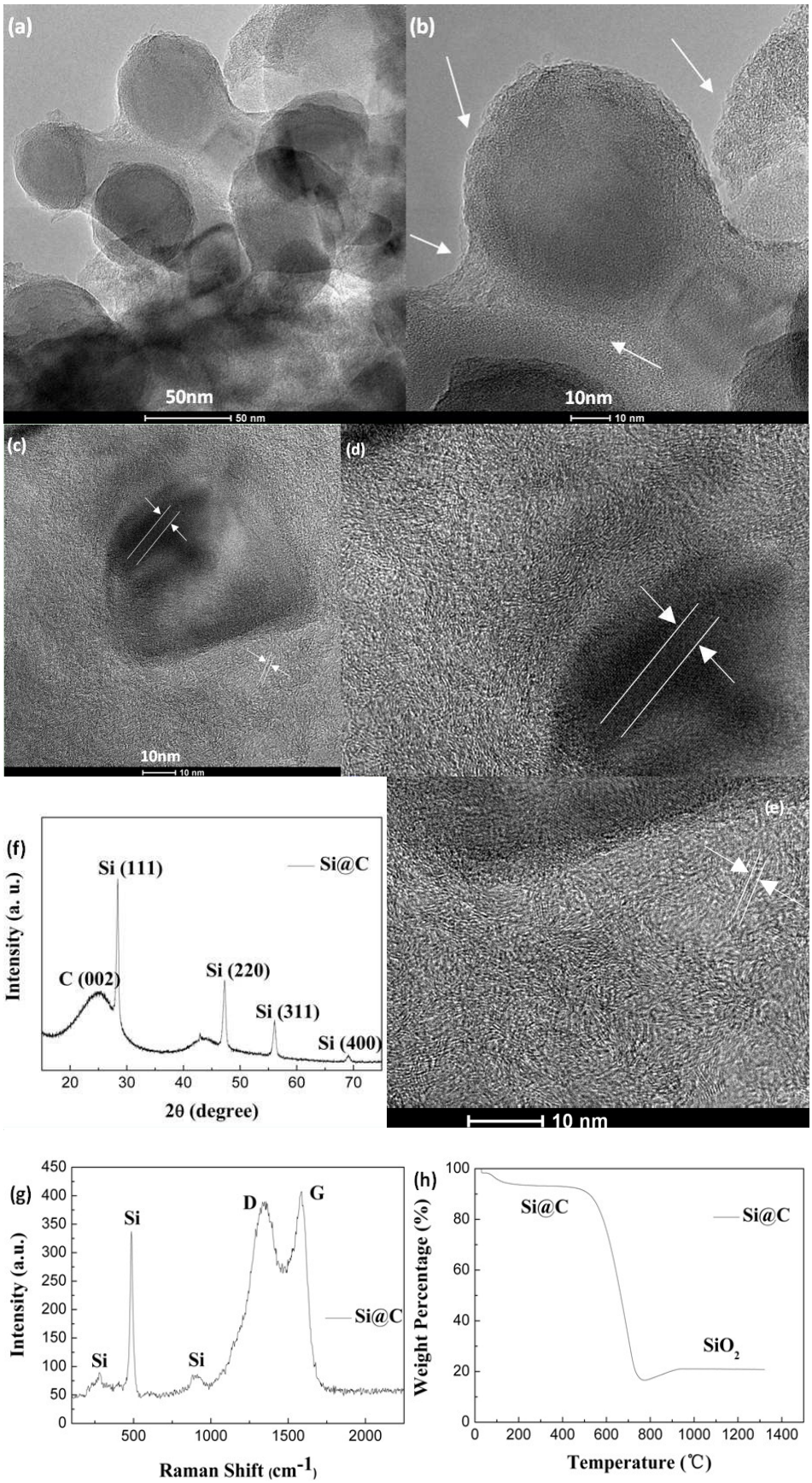

Fig. 2. The characterization of the prepared Si@C anode material. (a) TEM image of the Si@C material, (b) the high-magnification observation at the same location of (a), (c) TEM image showing the over-all structure of the Si@C material, (d) and (e) structure details of (c) with enlarged scale, (f) XRD pattern, (g) Raman spectrum, (h) TG curve. The structure shown in (c) can be further referred to Fig. S1.

Fig. 2g is the Raman spectrum of the Si@C material. Three peaks below 1000 cm^{-1} are ascribed to Si nanoparticles. Two peaks at 1347 and 1587 cm^{-1} correspond to the D band of disordered carbon and the G band of graphitized carbon, respectively. The I_D/I_G ratio of 0.95 implies a higher graphitization degree of the anode material, which was benefited from the cyclization reaction of PAN in the preparation process [6]. The higher graphitization degree is helpful to improve the electrical conductivity of the electrode material. The G peak is higher than the D peak, and it proved the existence of turbostratic graphite-like carbon furtherly.

The TG curve of the Si@C material was scanned under air atmosphere, from room temperature to 1200 ℃ at a heating rate of 10 ℃ min^{-1}. In the TG curve of Fig. 2h, there is a 21% weight platform after 938 ℃. The residue is white powder of SiO_2. The Si content of 9.8 w% is calculated according to the stoichiometric ratio of SiO_2. Based on the PAN/Si ratio of 20/1 (w/w), the carbon yield of this preparation method is 45.1%, consistent with the carbon yield of PAN-based carbon fiber (47.2%) [25].

Fig. 3 is the electrochemical performance of the prepared Si@C anode material. Fig. 3a shows CV curves of the Si@C material. In the first cathodic half-cycle

(discharge), the segment between 0.96 V and 0.45 V may correspond to the formation of the SEI film, which leads to an initial irreversible capacity of the battery [24]. At 0.14 V, there is a very weak peak of lithium intercalation into Si (Si→Li_xSi). Fig. 3b is the detail of Fig. 3a with enlarged scale. In the anodic half-cycle (charge), 0.75 V correspond to an anodic peak of lithium deintercalation from Si (Li_xSi → Si). The redox peaks are weak, which is attributed to only 6.9 w% of Si in the working electrode material. The increasing CV curve area is due to initial activation of the anode material, enabling more lithium to react with Si [6]. Fig. 3c shows the EIS result of the Si@C material. The EIS curve includes two semicircles and a linear diffusion drift. The first semicircle may correspond to the formation of the SEI film, and the second semicircle is probably because of the interfacial charge transfer impedance. The linear diffusion segment indicates that the three-dimensional conductive network formed by PAN-based turbostratic graphite-like carbon facilitates the diffusion and transport of lithium ions between the electrode and the electrolyte, thus reducing the diffusion resistance of lithium ions [24]. The impedance in the EIS curve is very small, equivalent to that of composite electrode materials about Si/carbon nanocoils [24] and Si/grapheme [26]. It shows that the PAN-based turbostratic graphite-like carbon formed a good conductive network in the Si@C anode material.

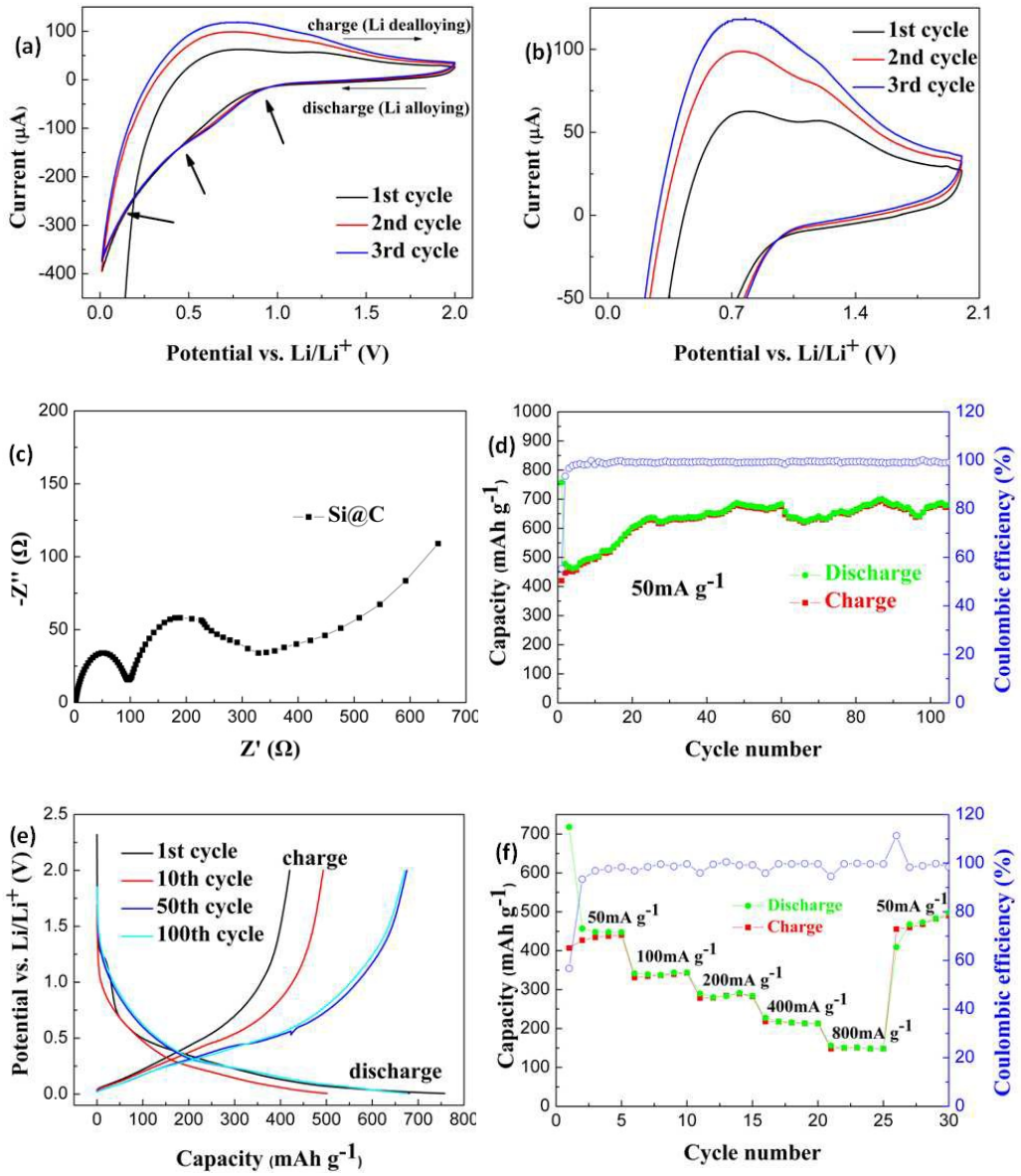

Fig. 3. The electrochemical performance of the prepared Si@C anode material. (a) CV curves, (b) detail of (a) with enlarged scale, (c) EIS curve, (d) cycling performance, (e) voltage-capacity curve, (f) rate capability. The EIS curve of the pure Si can be further referred to Fig. S2.

The cycling performance test was conducted with a constant current charge and discharge of 50 mA g^{-1}. As shown in Fig. 3d, the first discharge capacity was 757 mAh g^{-1} with the Coulombic efficiency of 55%. Then, the charge-discharge capacity increased gradually, and the Coulombic efficiency reached above 99%. The charge-discharge capacity was up to 700 mAh g^{-1}, slightly dropped to 640 mAh g^{-1}, and mostly in 680 mAh g^{-1}. The cell capacity of this anode material is about twice as that of the commercial anode material in LIBs at present, and it is important that the Si content is only 9.8 w% in the Si@C anode material. There is no report about the anode material, similar to this Si@C material with the special structure, which can be give full play to the anode performance of Si. With regard to the Si@C anode material with the yolk-shell structure, the 65 w% Si content in the anode material corresponded to the initial reversible capacity of 1346 mAh g^{-1} in Wang's work [6], while the 77 w% Si content corresponded to the reversible capacity of 2350 mAh g^{-1} in Cui's work [15]. The anode performance of Si was not played fully in the yolk-shell structure material, and it may be that some pulverized Si nanoparticles can not keep a good contact with the carbonaceous shell.

Fig. 3e shows the voltage-capacity curve in the charge-discharge process. There is a discharge platform of 0.16 V in the discharge segments. The shape of the discharge curve in the first cycle is different from other subsequent discharge curves, due to that the electrolyte formed the SEI films on the surface of electrode materials. The charge curves indicate that the cell capacity increased, and the capacity of the 50^{th} cycle was basically the same with that of the 100^{th} cycle. Fig. 3f is the rate capability

of the Si@C anode material. The cell capacity could recover after the large current charge-discharge, which indicated its good rate capability.

In this study, the charge-discharge capacity of the Si@C material increased rather than decreased with the increase of cycling numbers. As indicated in Fig. 4, the phenomenon can be interpreted as: with the increase of charge-discharge cycles, the uniformly-coated Si nanoparticles continued to pulverize into Si particles with a smaller size, and made the further increase of their lithium-intercalation ability. The three-dimensional network formed by PAN-based turbostratic graphite-like carbon was robust enough to accommodate the expansion-contraction of Si nanoparticles; moreover, the good electrical conductivity of the carbonaceous matrix could make the further pulverized Si nanoparticles still keeping contact with the electrode material on the whole. The turbostratic structure also made that the further pulverized Si nanoparticles were not easy to reunite. At the same time, lithium ions could diffuse and transfer quickly in the carbonaceous matrix, which supported by the EIS result. As for the slight drop of the charge-discharge capacity, it may be resulted from the small amount aggregation of the further pulverized Si nanoparticles in the charge-discharge cycles. According to the weight ratio of the Si@C material, and combined with the theory capacity of graphite and Si, the theory capacity of the anode material was calculated to be 686 mAh g^{-1} in this study. From the actual capacity of the battery, the structure design of the anode material gave full play to the electrochemical performances of nanoscale Si and the PAN-based carbonaceous matrix.

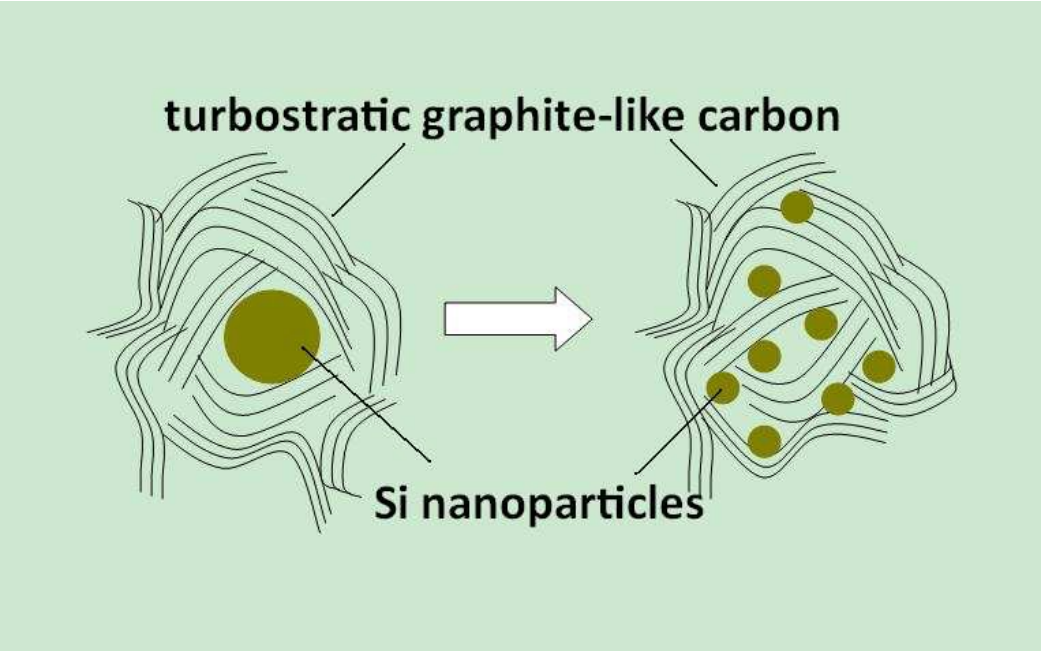

Fig. 4. The schematic diagram of structure change about the Si@C anode material in the charge-discharge process.

In order to further understand the excellent capacity and rate capability of the Si@C material, the morphology of the working electrode in the lithium-intercalation and lithium-deintercalation process was studied by SEM. Fig. 5a is the SEM image of the working electrode before the battery test, Fig. 5b and 5c are its element mapping pictures. It can be seen that Si nanoparticles uniformly distributed in the carbonaceous matrix. Fig. 5d shows that a SEI layer coated on the electrode material after 100 cycles [24]. Fig. 5e and 5f are TEM images of the working electrode after 100 cycles. As shown in TEM images, the particle size of Si decreased sharply to below 10 nm. It is the most direct evidence that the Si@C material could give full play to the lithium-intercalation ability of nanoscale Si, and thus improve the battery capacity. In addition, according to the lattice fringes in TEM images (arrows), the robust

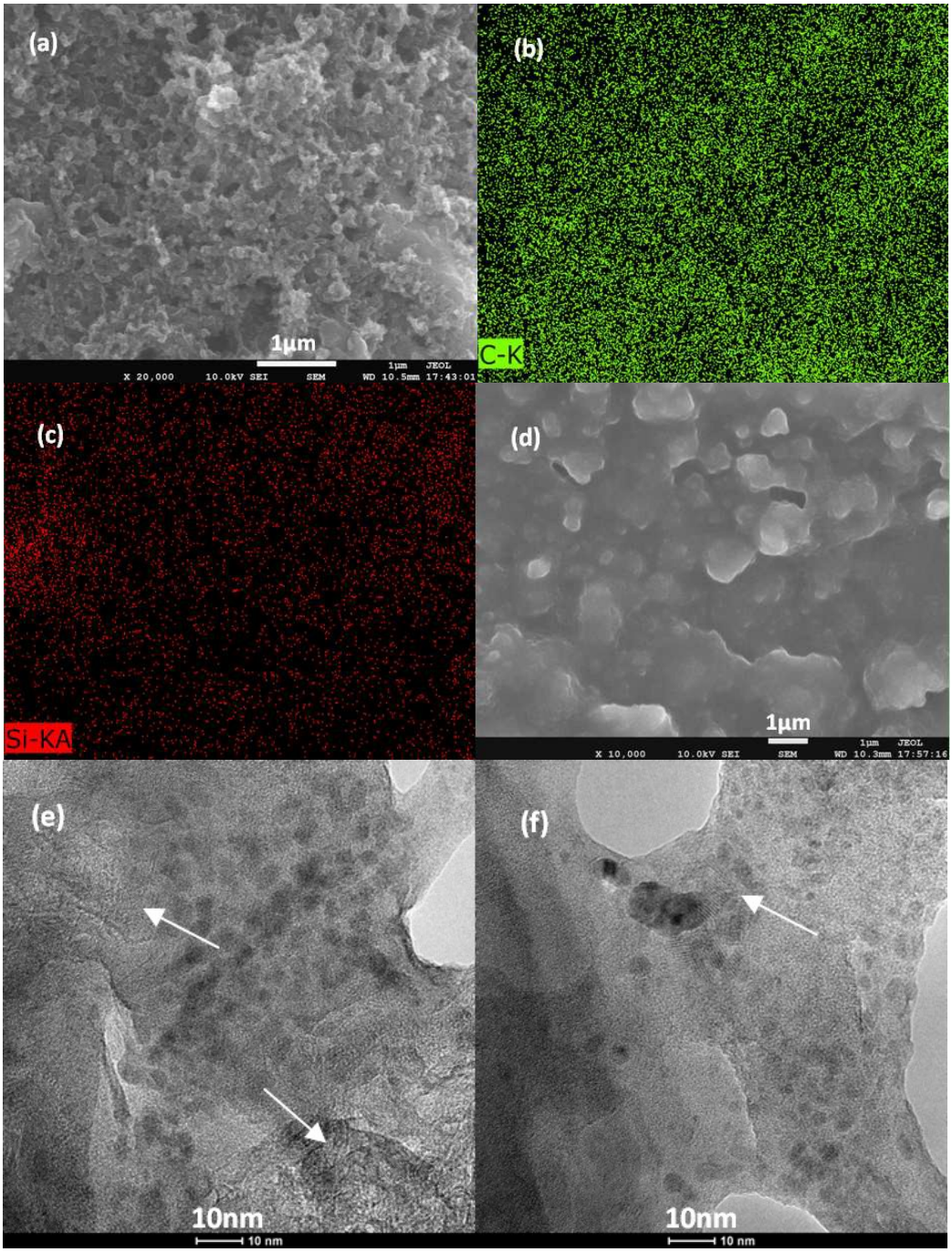

Fig. 5. The microstructure of the working electrode material before and after the battery test. (a) SEM image before test, (b) and (c) the element mapping pictures of (a), (d) SEM image after test, (e) and (f) TEM images after test, lattice fringes indicated by arrows can be further referred to Fig. S3 and S4.

carbonaceous matrix formed by PAN-based turbostratic graphite-like carbon could not only accommodate the expansion-contraction of Si nanoparticles to maintain the integrity of the electrode, but also make the pulverized Si nanoparticles to keep good contact with the working electrode, thus to enable the full lithiation of Si and improve the battery capacity.

4. Conclusion

In conclusion, the anode material of Si nanoparticles wrapped in PAN-based turbostratic graphite-like carbon was prepared. The carbonaceous matrix formed by PAN-based turbostratic graphite-like carbon could not only accommodate the expansion-contraction of Si nanoparticles, but also make the pulverized Si nanoparticles (<10nm) to keep good contact with the working electrode. Moreover, lithium ions could diffuse and transfer quickly in the PAN-based carbonaceous matrix. As a result, the capacity of the Si@C anode material reached 680 mAh g^{-1}, about twice as that of the commercial anode material, with only 9.8 w% Si content. The preparation method of the Si@C material is very simple and effective, easy to mass production. The prepared PAN-based carbonaceous matrix with this special structure has a great potential to be widely used in the preparation of Si-based anode materials.

Acknowledgment

The authors would like to acknowledge the support of the National Natural Science Foundation of China (no. 51303199) for funding this research work.

References

[1] X. Su, Q. L. Wu, J. C. Li, X. C. Xiao, A. Lott, W. Q. Lu, B. W. Sheldon, J. Wu, Silicon-Based Nanomaterials for Lithium-Ion Batteries: A Review, Advanced Energy Materials, 2014, DOI: 10.1002/aenm.201300882.

[2] D. M. Piper, J. H. Woo, S.-B. Son, S. C. Kim, K. H. Oh, S.-H. Lee, Hierarchical Porous Framework of Si-Based Electrodes for Minimal Volumetric Expansion, Adv. Mater., 26 (2014) 3520-3525.

[3] H. Zhang, X. Qin, J. Wu, Y.-B. He, H. Du, B. Li, F. Kang, Electrospun core-shell silicon/carbon fibers with an internal honeycomb-like conductive carbon framework as an anode for lithium ion batteries, Journal of Materials Chemistry A, 3 (2015) 7112-7120.

[4] N. A. Kaskhedikar, J. Maier, Lithium Storage in Carbon Nanostructures, Adv. Mater., 21 (2009) 2664-2680.

[5] W. W. Lee, J.-M. Lee, Novel synthesis of high performance anode materials for lithium-ion batteries (LIBs), Journal of Materials Chemistry A, 2 (2014) 1589-1626.

[6] C. Pang, H. Song, N. Li, C. Wang, A strategy for suitable mass production of a hollow Si@C nanostructured anode for lithium ion batteries, Rsc Advances, 5 (2015) 6782-6789.

[7] J. Deng, H. Ji, C. Yan, J. Zhang, W. Si, S. Baunack, S. Oswald, Y. Mei, O. G. Schmidt, Naturally Rolled-Up C/Si/C Trilayer Nanomembranes as Stable Anodes for

Lithium-Ion Batteries with Remarkable Cycling Performance, Angewandte Chemie International Edition, 52 (2013) 2326-2330.

[8] B. Wang, T. Qiu, X. Li, B. Luo, L. Hao, Y. Zhang, L. Zhi, Synergistically engineered self-standing silicon/carbon composite arrays as high performance lithium battery anodes, Journal of Materials Chemistry A, 3 (2015) 494-498.

[9] H. Kim, M. Seo, M.-H. Park, J. Cho, A Critical Size of Silicon Nano-Anodes for Lithium Rechargeable Batteries, Angewandte Chemie International Edition, 49 (2010) 2146-2149.

[10] M. H. Park, M. G. Kim, J. Joo, K. Kim, J. Kim, S. Ahn, Y. Cui, J. Cho, Silicon Nanotube Battery Anodes, Nano Letters, 9 (2009) 3844-3847.

[11] C. K. Chan, H. L. Peng, G. Liu, K. McIlwrath, X. F. Zhang, R. A. Huggins, Y. Cui, High-performance lithium battery anodes using silicon nanowires, Nat. Nanotechnol., 3 (2008) 31-35.

[12] S. H. Ng, J. Z. Wang, D. Wexler, K. Konstantinov, Z. P. Guo, H. K. Liu, Highly reversible lithium storage in spheroidal carbon-coated silicon nanocomposites as anodes for lithium-ion batteries, Angew. Chem.-Int. Edit., 45 (2006) 6896-6899.

[13] Y. S. Jung, K. T. Lee, S. M. Oh, Si-carbon core-shell composite anode in lithium secondary batteries, Electrochim. Acta, 52 (2007) 7061-7067.

[14] Y. Hwa, W. S. Kim, S. H. Hong, H. J. Sohn, High capacity and rate capability of core-shell structured nano-Si/C anode for Li-ion batteries, Electrochim. Acta, 71 (2012) 201-205.

[15] N. Liu, Z. Lu, J. Zhao, M. T. McDowell, H.-W. Lee, W. Zhao, Y. Cui, A pomegranate-inspired nanoscale design for large-volume-change lithium battery anodes, Nat. Nanotechnol., 9 (2014) 187-192.

[16] T. Yang, R. Zhou, D.-W. Wang, S. P. Jiang, Y. Yamauchi, S. Z. Qiao, M. J. Monteiro, J. Liu, Hierarchical mesoporous yolk-shell structured carbonaceous nanospheres for high performance electrochemical capacitive energy storage, Chemical Communications, 51 (2015) 2518-2521.

[17] D. Li, C. Lu, G. Wu, Y. Yang, Z. Feng, X. Li, F. An, B. Zhang, Heat-induced Internal Strain Relaxation and its Effect on the Microstructure of Polyacrylonitrile-based Carbon Fiber, Journal of Materials Science & Technology, 30 (2014) 1051-1058.

[18] L. Shen, L. Shen, Z. Wang and L. Chen, In Situ Thermally Cross-linked Polyacrylonitrile as Binder for High-Performance Silicon as Lithium Ion Battery Anode, Chemsuschem, 7 (2014) 1951-1956.

[19] L. Gong, N. Minh Hien Thi and E.-S. Oh, High polar polyacrylonitrile as a potential binder for negative electrodes in lithium ion batteries, Electrochemistry Communications, 29 (2013) 45-47.

[20] E. Frank, F. Hermanutz, M. R. Buchmeiser, Carbon Fibers: Precursors, Manufacturing, and Properties, Macromolecular Materials and Engineering, 297 (2012) 493-501.

[21] X. Z. Dong, C. X. Lu, P. C. Zhou, S. C. Zhang, L. Y. Wang, D. H. Li, Polyacrylonitrile/lignin sulfonate blend fiber for low-cost carbon fiber, RSC Adv., 5 (2015) 42259-42265.

[22] L. Z. Zhang, C. X. Lu, Y. G. Lu, G. P. Wu, F. He, The structure and thermal performance of PAN fibers during oxidative stabilization, New Carbon Materials, 20 (2005) 144-150.

[23] Y. F. Wen, X. Cao, Y. G. Yang, H. Li, J. Q. Guo, L. Liu, Carbonization of pre-oxidized polyacrylonitrile fibers, New Carbon Materials, 23 (2008) 121-126.

[24] L. Y. Wang, Q. G. Guo, J. Z. Wang, H. Li, G. Z. Wang, J. H. Yang, Y. Song, Y. Qin, L. Liu, Improved cycling performance of a silicon anode for lithium ion batteries using carbon nanocoils, RSC Adv., 4 (2014) 40812-40815.

[25] F. He, Carbon Fiber and Its Application Technology, Chemical Industry Press, Beijing, 2004.

[26] H. Li, C. Lu, B. Zhang, A straightforward approach towards Si@C/graphene nanocomposite and its superior lithium storage performance, Electrochim. Acta, 120 (2014) 96-101.

Table of contents

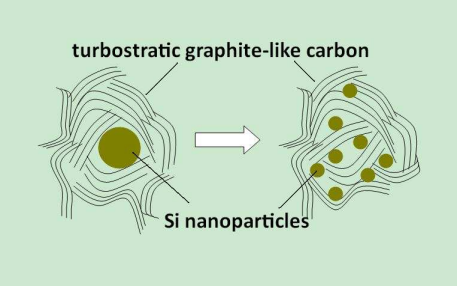

The carbonaceous matrix formed by PAN-based turbostratic graphite-like carbon could give full play to the lithium-intercalation ability of Si nanoparticles.